Comparative Assessment of Image Fusion Methods for Land Cover/ Land Use Monitoring

R Prema, M G Sumithra

Abstract — Land Cover/Land Use (LCLU) applications includes rural/urban change detection, biomass mapping and natural resource management. The high spatial and high spectral resolution are necessary for efficient class discrimination of LCLU monitoring and mapping. The multispectral (MS) images acquired from land observation satellites like Landsat, MODIS and IRS etc. are able to provide only coarse spatial resolution. The Panchromatic (PAN) band in satellite images have high spatial but coarse spectral resolution. The process of combining PAN and MS band images to produce high spatial and spectral resolution is called Image Fusion. Classical image fusion algorithms are Brovey, Intensity Hue and Saturation (IHS), Principal Component Analysis (PCA), High Pass Filtering (HPF), Atrous Wavelet Transform (ATWT) and Generalized Laplacian Pyramid (GLP). These benchmarking methods are coming under pixel level fusion. In this paper, we are going to analyze the performance quantitatively using evaluation parameters Spectral Angle Mapper (SAM), Universal Image Quality Index (UIQI) and Relative Global-dimensional Synthesis Error (ERGAS). The experiment is performed using datasets Landsat and QuikBird. All the simulations were carried out in MATLAB R2014a. Comparison of all the methods concludes the better approach for future research.

Keywords—Image Fusion, Land Cover/Land Use, Pixel level fusion, Spatial resolution and Spectral Resolution

I. INTRODUCTION

Remote sensing is the acquisition of earth surface information without making physical contact with that object. It is the most cost effective and efficient technique that provide unique perspective to class discrimination of LCLU. For Rural/Urban change detection (LC) and Biomass mapping (LU) applications we are in need of high resolution image to obtain detailed information together with multispectral data to identify fine distinction between various classes. The available panchromatic band (PAN) with high spatial resolution and Multispectral band (MS) with high spectral resolution in remote sensing satellites like Landsat ETM + (Enhanced Thematic Mapper), IRS, MODIS (Moderate Resolution Imaging Spectroradiometer), IKONOS etc. satisfy the requirement of LCLU. But the presence of PAN and MS bands are not sufficient to provide the necessary information for detecting Urbanization and Deforestation processes. Therefore, we are in need of Image Fusion methods to combine high spatial resolution PAN with high spectral resolution MS to produce MS with high spatial and spectral resolution. The benchmarking image fusion algorithms are Brovey, Intensity Hue and Saturation (IHS), Principal Component Analysis (PCA), High Pass Filtering (HPF), Atrous Wavelet Transform (ATWT) and Generalized Laplacian Pyramid (GLP). Four indices were used for quantitative evaluation including SAM, UIQI, CC and ERGAS for the comparison of aforementioned methods.

II. SATELLITE IMAGE CHARACTERISTICS

Satellite image is characterized by its resolution. The types are

1) Spatial
2) Spectral
3) Temporal
4) Radiometric

Based on Spectral resolution, the bands have been classified into the following types,

5) *Panchromatic Band*
   - It operates in unique band
   - The sensor that integrates Visible light and Near Infrared
   - Wavelength in the order of 100's of nm
   - Poor spectral resolution
   - High spatial resolution
6) *Multispectral Bands*
   - It consists of three spectral bands in visible region
   - Wavelength in the order of 50's of nm
   - Poor spatial resolution
   - High spectral resolution
7) *Superspectral Bands*
   - Number of bands is greater than 10
8) *Hyperspectral Bands*
   - Wavelength in the order of 10's of nm
   - Number of bands is greater than 100
9) *Ultraspectral Bands*
   - Wavelength in the order of 1 nm

Radiometric Resolution

For 8 bits: $2^8 = 256$ Colors
For 3 bits: $2^3 = 8$ Colors

Temporal Resolution

It refers to the revisiting frequency of a satellite sensor for a specific location.

Revised Manuscript Received on December 22, 2018.

R Prema, Assistant Professor, Department of ECE, Bannari Amman Institute of Technology, Sathyamangalam,TamilNadu, India (Email: prema@bitsathy.ac.in)

M G Sumithra, Professor, Department of ECE, Bannari Amman Institute of Technology, Sathyamangalam, TamilNadu, India (Email: sumithramg@bitsathy.ac.in)

III. IMAGE FUSION

Image Fusion combines geometrically registered Multispectral and Panchromatic band to produce fine spatial and fine spectral resolution image. The techniques involved are categorized into Pixel, Feature and Decision level.

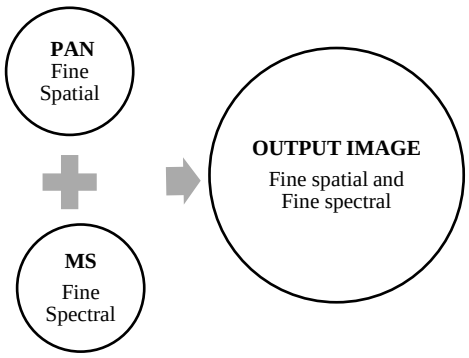

Fig 1. Image Fusion

A. Pixel level Fusion

It refers to low level. By combining pixels from different images, the resultant image is produced by using Component Substitution (Spatial) and Multiresolution (Spectral) algorithms.

B. Feature level Fusion

It refers to intermediate level. The features like textures, edges, shape, tone and shadow are extracted from one source and fused with different source to produce resultant image.

C. Decision level Fusion

It refers to high level. The images are processed separately to obtain information and based on the collected information decision rules are made.

IV. METHODS

Ideal image fusion method should preserve spectral characteristics and must be able to add spatial characteristics to the image. The MS and PAN images should have been registered properly to avoid misalignment. Because misregistration is major source of error in Image Fusion. In this paper we are going to carry out detailed assessment about pixel level fusion methods. Pixel level fusion is further classified into Component Substitution and Multiresolution analysis methods.

A. Component Substitution Methods (CS)

1) Brovey Transform (BT)

It is based on chromaticity transform [1]. It is a simple method which combines arithmetic and normalization operations. It transforms all luminance information into a panchromatic image of high resolution. The simplified equation is given in (1)

$$\widehat{MS}_{HR} = (\widehat{MS}_{UP} * PAN)/\sum MS_{UP} \quad (1)$$

Where $\widehat{MS}_{HR}$ = Pansharpened Image, PAN = Panchromatic Image, $\widehat{MS}_{UP}$ = MS upsampled to PAN Scale and $\sum MS_{UP}$ = (MS_{B1} + MS_{B2} +MS_{B3}) /3

2) Intensity, Hue Transform and Saturation (IHS)

Human visual cognitive system tends to treat Intensity (Luminance/Brightness), Hue (Tone of the Color) and Saturation (Purity of the color) as orthogonal perceptual axes. The IHS method [2] exploits this property and converts RGB to IHS. Fast IHS [3] [4] and Generalized IHS [5] are fast and easy implementation methods, which avoid direct transformation, substitution and reverse transformation. The RGB to IHS forward transformation is given by (2),

$$\begin{bmatrix} I \\ V1 \\ V2 \end{bmatrix} = \begin{bmatrix} \frac{1}{3} & \frac{1}{3} & \frac{1}{3} \\ \frac{-1}{\sqrt{6}} & \frac{-1}{\sqrt{6}} & \frac{2}{\sqrt{6}} \\ \frac{1}{\sqrt{6}} & \frac{-1}{\sqrt{6}} & 0 \end{bmatrix} \begin{bmatrix} MS_{UP\,B1} \\ MS_{UP\,B2} \\ MS_{UP\,B3} \end{bmatrix} \quad (2)$$

Where

H= $\tan^{-1}$[V2/V1] and S=$\sqrt{V1^2 + V2^2}$

$$\begin{bmatrix} MS_{HR\,B1} \\ MS_{HR\,B2} \\ MS_{HR\,B3} \end{bmatrix} = \begin{bmatrix} 1 & \frac{-1}{\sqrt{6}} & \frac{3}{\sqrt{6}} \\ 1 & \frac{-1}{\sqrt{6}} & \frac{-3}{\sqrt{6}} \\ 1 & \frac{2}{\sqrt{6}} & 0 \end{bmatrix} \begin{bmatrix} PAN \\ V1 \\ V2 \end{bmatrix} \quad (3)$$

The backward transformation from IHS to RGB is given in (3). The generalized IHS is given by (4)

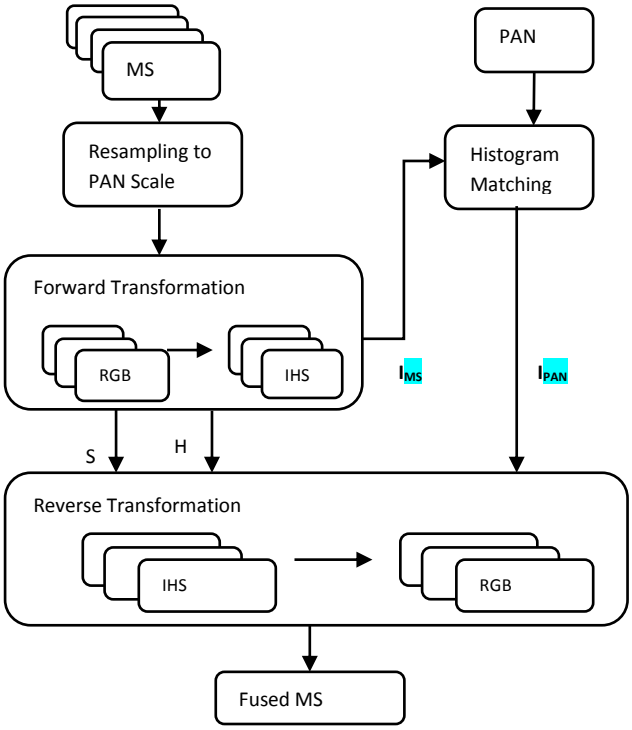

Fig 2. A. Component Substitution Methodology

$$\begin{bmatrix} MS_{HR\,B1} \\ MS_{HR\,B2} \\ MS_{HR\,B3} \end{bmatrix} = \begin{bmatrix} MS_{UP\,B1} \\ MS_{UP\,B2} \\ MS_{UP\,B3} \end{bmatrix} + (PAN - \sum MS_{UP}) \quad (4)$$

Where $MS_{HR\ (B1-B3)}$ = Pansharpened Image and $MS_{UP\ (B1-B3)}$ = MS upsampled to PAN Scale.

3) Principal Component Analysis (PCA)

PCA is achieved through linear transformation of data i.e., multi-dimensional rotation of the data. As Gonzalez et al [2] proposed this statistical procedure transforms the number of correlated variables into number of uncorrelated variables known as Principal Components (PC). The first component account for the maximum variability in the data as possible. Each succeeding components accounts for the remaining variability as possible. The benefits of PCA method (Hotelling Transform/ Karhunen-Loeve Transform) includes decorrelation of multi spectral data and compression/reduction of variance. It incorporates decorrelation technique, i.e., reduces auto correlation within the signal and cross correlation within a set of signals while preserving the other spectral aspects of the signal. Main advantage is the dimensionality reduction technique applied in this method is independent of the number of bands selected for analysis. In general, there are two types of PCA based on the calculation of covariance and correlation matrices, first one implies unstandardized PCA and latte implies standardized PCA.

The PCA's comprises calculation of covariance/correlation matrix, eigen vectors/matrices and PC's. By histogram matching first PC (from low resolution MS) is replaced by the high resolution PAN (after equalization with MS) image. Then inverse PCA to get the original image. As Gillespie et al [1] mentioned PCA is data dependent, therefore coefficients change from scene to scene it leads to computation expensive. In Shahdoosti et al [6], instead of variance the parameters like skewness, kurtosis and infinite order statistics are also analyzed.

The forward and backward transformation for PCA is given in (5) and (7)

$$\widehat{PC} = \widehat{W_{PC}}\ \widehat{MS_{UP}} \tag{5}$$

$$\widehat{PC} = \begin{bmatrix} PC_1 \\ PC_2 \\ \vdots \\ PC_n \end{bmatrix} \qquad \widehat{W_{PC}} = \begin{bmatrix} e_{11} & \cdots & e_{1n} \\ \vdots & \ddots & \vdots \\ e_{n1} & \cdots & e_{nn} \end{bmatrix} \tag{6}$$

$$\widehat{MS_{HR}} = \begin{bmatrix} e_{11}e_{21}\ldots e_{n1} \\ e_{12}e_{22}\ldots e_{n2} \\ \vdots\ \vdots\ \ldots\ \vdots \\ e_{1n}e_{2n}\cdots e_{nn} \end{bmatrix} \begin{bmatrix} PAN \\ PC_2 \\ \vdots \\ PC_n \end{bmatrix} \tag{7}$$

The generalized standardization PCA is given by (8)

$$\begin{bmatrix} MS_{HR\,B1} \\ MS_{HR\,B2} \\ MS_{HR\,B3} \end{bmatrix} = \begin{bmatrix} MS_{UP\,B1} \\ MS_{UP\,B2} \\ MS_{UP\,B3} \end{bmatrix} + (\text{PAN-}PC_1) \begin{bmatrix} e_{11} \\ \vdots \\ e_{n1} \end{bmatrix} \tag{8}$$

Where $\widehat{W_{PC}}$ = Transformation matrix contains *e* Eigen vectors.

B. Mutiresolution Analysis Methods (MRA)

4) High Pass Filtering (HPF)

The spatial information is present in the high frequency content of PAN. Therefore, the objective of HPF [7] [8] is to extract high frequency information from PAN and inject that into the upsampled version of MS. The high frequency information can be computed by two ways, first one is by filtering the high resolution PAN with high pass filter (HPF) and latter method is by filtering the original PAN with low pass filter (LPF) and then subtract the original PAN from low pass filtered version of PAN to extract the high frequency details. This method preserves more percentage of spectral characteristics. But it introduces spatial distortion in the fused image. Popular methods in filtering techniques are High Pass Filter Additive (HPFA) [9] [10] and High Frequency Modulation (HPM) it is also known as Smoothing Filter based Intensity Modulation (SFIM) [11] [12]. The simplified mathematical equation is given by (9)

$$\widehat{MS_{HR}} = \widehat{MS_{UP}} + (PAN_{HR} - PAN_{LR}) \tag{9}$$

Where PAN_{LR} = PAN*h_o, h_o is the low pass filter like averaging filter.

5) Atrous Wavelet Transform (ATWT)

Wavelet method is based on decomposition of image based on the frequency content [13]. It provides resolution in both frequency and space domain. The wavelet transform is described as,

$$W(a,b) = \frac{1}{\sqrt{a}} \int_{-\infty}^{\infty} f(t) \frac{\varphi(t-b)}{a} dt \tag{10}$$

Where *a* and *b* are scaling and translational parameters in (10). Wavelet merging fusion can be done methods like decimated, undecimated and ATWT. Undecimated transformation is achieved by using Mallat's algorithm, but it is not shift invariant. ATWT [14] [15] is translation invariant and it is the very effective method the recent approaches. The image *p* is decomposed into wavelet planes w_j as in (11) and the reconstruction is defined as in (12)

$$w_j = p_{j-1} - p_j \quad j = 1, \ldots r \tag{11}$$

$$p = p_r + \sum_{j=1}^{r} w_j \tag{12}$$

Where r = level of decomposition. The above sequence can be calculated by using B3 spline dyadic wavelet scaling function as h_o= 1/16[1 4 6 4 1], which is also referred by names like atrous filter, Starck & Murtagh (S&M) filter [9]. The generalized equation is given by (13),

$$\widehat{MS_{HR}} = \widehat{MS_{UP}} + (PAN_{HR} - PAN_{LR}) \tag{13}$$

Where $PAN_{LR} = p_r$, p_r is the approximation of PAN image at decomposition level r.

6) Generalized Laplacian Pyramid (GLP)

Laplacian Pyramid [16] is defined as convolving original image with Gaussian-like weighting functions. For each level, the band limit is reduced to one octave level, therefore the decomposition is similar to passing the original image to LPF and the resultant image is referred as Gaussian pyramid. The image size and spatial resolution are reduced

Published By:
Blue Eyes Intelligence Engineering
& Sciences Publication

to half at each level in GLP whereas in ATWT, only spatial resolution is reduced for each level but size of the image is kept constant [17]. The procedure for obtaining GLP [4] is as follows as,

- Constructing image pyramid from MS
- Convolving the above pattern with the target pattern (image pyramid of PAN) with each level
- The obtained correlation values are filtered through intensity transformation
- The final step is locally integrating values with Gaussian density function

The generalized form of mathematical model is given in (14)

$$\widehat{MS}_{HR} = \widehat{MS}_{UP} + (PAN_{HR} - PAN_{LR} \frac{)cov(\widehat{MS}_{UP}, PAN_{LR})}{var(PAN_{LR})} \quad (14)$$

Where PAN_{LR} = PAN*h_o, h_o is the Gaussian filter.

V. EVALUATION PARAMETERS

Generally quality assessment in image fusion is based on three approaches, which are Quality indices considered without reference image, Wald's Protocol and Quality indices considered with reference image.

In this paper, we are going to consider first approach for our evaluation. The parameters are,

A. Spectral angle mapper(SAM)

It is defined as the estimation of angle between corresponding pixels of reference images and fused images [18].

$$SAM(\boldsymbol{I}_{\{i\}}, \boldsymbol{J}_{\{j\}}) = \arccos\left(\frac{\langle I_{\{i\}}, J_{\{j\}}\rangle}{\|I_{\{i\}}\| \, J_{\{j\}}\|}\right) \quad (15)$$

Where, $\langle \boldsymbol{I}_{\{i\}}, \boldsymbol{J}_{\{j\}}\rangle$ is the inner product, $\|I_{\{i\}}\|$ is the vector l_2 norm in (15). For whole image, SAM is calculated by averaging single measures over the all pixels. The optimal index value of the SAM is zero, which specifies no spectral distortion between the images.

B. The Root Mean Square Error (RMSE)

It is the standard quality measure between reference and resultant fused images.

$$RMSE\ (\boldsymbol{I}, \boldsymbol{J}) = \sqrt{E[(\boldsymbol{I} - \boldsymbol{J})^2]} \quad (16)$$

When **I**=**J**, RMSE will be zero which is the ideal value.

C. The Relative Global-dimensional Synthesis Error (ERGAS)

The most credited evaluation performance metric for image fusion is ERGAS [19], it is defined as

$$ERGAS = \frac{100}{R} \sqrt{\frac{1}{N}\sum_{k=1}^{N} \frac{RMSE(\boldsymbol{I}_k \boldsymbol{J}_k)^2}{\mu(\boldsymbol{I}_k)}} \quad (17)$$

Where μ denotes the mean of the pixels and R denotes the ratio between PAN and MS. The optimal value is zero, since it is calculated by summing all the RMSE values.

D. Universal Image Quality Index (UIQI)

The scalar index is proposed in Wang et al [20], which overcomes the limitations of standard quality measurements such as mean squared error (MSE), Peak signal to noise ratio (PSNR), root mean squared error (RMSE), mean absolute error (MAE), and signal-to-noise ratio (SNR). The interpretation is given in (18)

$$Q\ (\boldsymbol{I}, \boldsymbol{J}) = \frac{\sigma_{IJ}}{\sigma_I \sigma_J} \frac{2\bar{I}\bar{J}}{((\bar{I})^2 + (\bar{J})^2)} \frac{2\sigma_I \sigma_J}{(\sigma_I{}^2 + \sigma_J{}^2)} \quad (18)$$

It is also referred as Q-Index. The value ranges from [-1, 1] and best fidelity to reference value is 1. For four spectral bands, the vectored form Q4-index and for more than four bands we have to follow the generalization of Q4 index which is denoted as $Q2^n$ index is mentioned in [21] [22] respectively.

VI. EXPERIMENTAL RESULTS AND DISCUSSION

Landsat and QuickBird satellite dataset has been used for assessment of benchmarking image fusion algorithms. The Landsat 7 ETM+ (Enhanced Thematic Mapper Plus) images has been taken from USGS (United States Geological Survey) [23] and the study area is Delhi, India. The experiments were analyzed using 30m MS (True Color Composite: Bands 3,2 and 1) and 15m PAN (Band 8). The QuickBird data set is taken from GLCF (Global Land Cover Facility) [24] and the study area is Sundarbans, Bangladesh. The experiments were analyzed using 2.4m MS and 0.61m PAN. The Landsat and QuickBird image is shown in Fig. 3. The comparison results of classical image fusion methods BT, IHS, PCA, HPF, ATWT and GLP for QuickBird and Landsat dataset are shown in Fig 4 and 5 respectively. The quantitative assessment for the above six methods has been listed in Table 1. The evaluation parameters UIQI, SAM and ERGAS are taken evaluation.

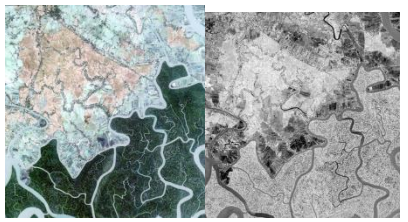

(a)

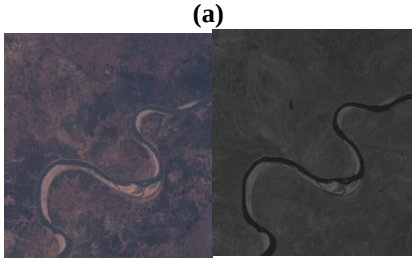

(b)

Fig 3. Datasets (a) 2.4 m Quickbird MS and PAN (b) 30m Landsat MS and PAN

(a) **(b)** **(c)**

Published By:
Blue Eyes Intelligence Engineering
& Sciences Publication

(d) (e) (f)

Fig 4. QuickBird Dataset: (a) BT (b) IHS (c) PCA (d) HPF (e) ATWT (f) GLP

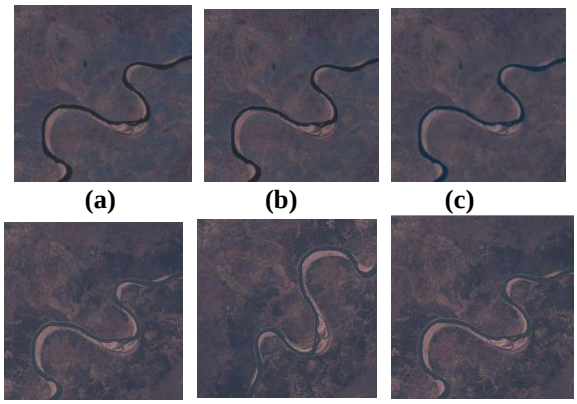

(a) (b) (c)

(d) (e) (f)

Fig 5. Landsat Dataset: (a) BT (b) IHS (c) PCA (d) HPF (e) ATWT (f) GLP

Table 1: Comparison of Evaluation Parameters – Landsat Dataset

Methods	Landsat	UIQI	SAM	ERGAS
CS	BT	0.351	1.3	0.00358
	IHS	0.347	1.52	0.00358
	PCA	0.389	3.12	0.00382
MRA	HPF	0.749	1.67	0.00213
	ATWT	0.746	1.71	0.00221
	GLP	0.784	1.61	0.00197

The quality indices Universal Quality Image Index (UIQI) is increasing towards 1.0 for better quality. The remaining evaluation parameters Spectral Angle Mapper (SAM) and Relative global dimensional synthesis error (ERGAS) are decreasing towards 0 for better accuracy. From the table 1 and 2, it has been observed that the MRA (HPF, ATWT and GLP) based methods are outperforming when compared to CS (BT, IHS and PCA) based methods.

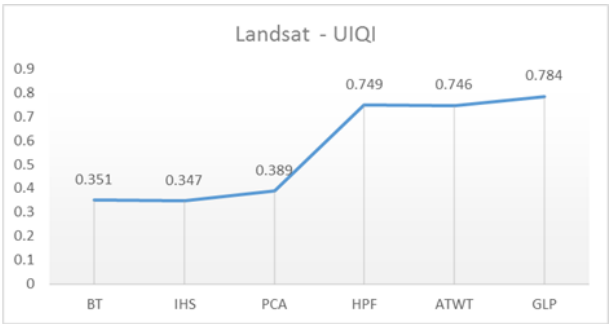

(a)

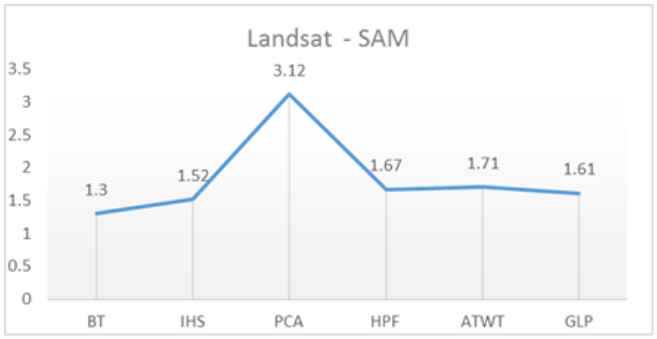

(b)

(c)

Fig 6. Landsat: (a) UIQI (b) SAM (c) ERGAS

The evaluation parameters UIQI, SAM and ERGAS has been plotted separately in the graph Fig 6 for the detailed reference of Landsat dataset. In Fig 6.a, UIQI values are approaching towards 1 in the MRA methods, therefore MRA methods give more fidelity comparing to the CS methods. SAM values in both the methods are not satisfactory, it shows that the resultant images are having more spectral distortion, refer Fig 6.b. For MRA methods ERGAS values are approaching towards zero as shown in Fig 6.c, infers that again MRA methods are outperforming than the CS methods.

Table 2: Comparison of Evaluation Parameters – QuickBird Dataset

Methods	QuickBird	UIQI	SAM	ERGAS
CS	BT	0.0972	19.3	0.0366
	IHS	0.0803	21.2	0.0295
	PCA	0.0797	21	0.0295
MRA	HPF	0.725	20	0.0104
	ATWT	0.714	20.1	0.0107
	GLP	0.813	18.8	0.00787

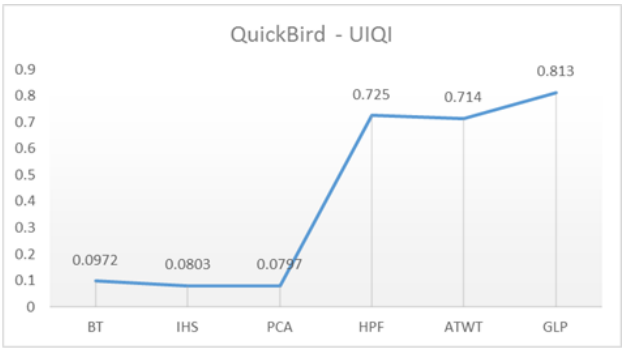

(a)

Published By:
Blue Eyes Intelligence Engineering
& Sciences Publication

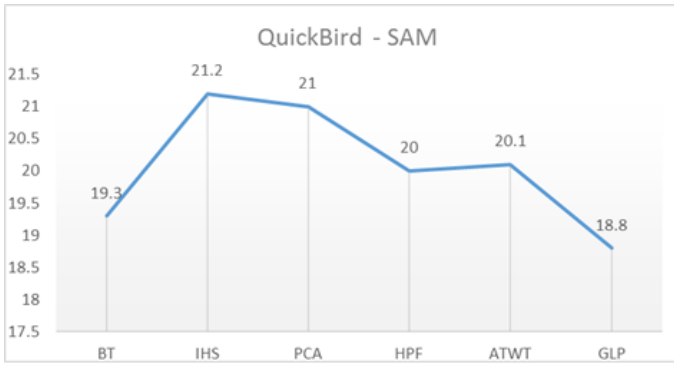

(b)

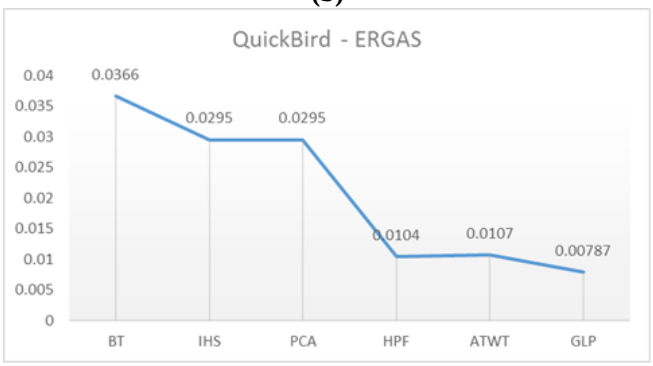

(c)

Fig 7. QuickBird: (a) UIQI (b) SAM (c) ERGAS

From the table 5.2, the evaluation parameters has been plotted in the graph Fig 7 for the detailed reference of Quickbird Dataset. The plots in Fig 7, clearly shows that MRA methods are having better performance in terms of UIQI and ERGAS. SAM values are not approaching towards zero, since spectral characteristics are having higher distortion in the resultant fused image.

CONCLUSION

From the assessment of CS and MRA methods, it has been inferred that besides the low computational effort and simplicity in CS, the MRA methods are providing better resultant images by preserving the detail information and maintaining the consistency all over the image. The hybrid methods can be implemented by fusing the ATWT and GLP methods with high pass modulation (HPM) and Gabour transform [25] to reduce the spectral distortion and minimize the error.

The analysis could be used as the basis for development, validation and analysis for the future research investigation including geostatistics based domain approaches including semi-variogram and cross-variogram models.

REFERENCES

[1] A. R. Gillespie, A. B. Kahle, and R. E. Walker, “Colour of correlated images—II. Channel ratio and ‘chromaticity’ transformation techniques,” Remote Sens. Environ., vol. 22, no. 3, pp. 343–365, 1987.

[2] P. S. Chavez, Jr., S. C. Sides, and J. A. Anderson, “Comparison of three different methods to merge multiresolution and multispectral data: Landsat TM and SPOT panchromatic,” Photogramm. Eng. Remote Sens., vol. 57, no. 3, pp. 295–303, Mar. 1991.

[3] B. Aiazzi, L. Alparone, S. Baronti, and A. Garzelli, “Context-driven fusion of high spatial and spectral resolution images based on oversampled multi-resolution analysis,” IEEE Trans. Geosci. Remote Sens., vol. 40, no. 10, pp. 2300–2312, Oct. 2002.

[4] H.R. Shahdoosti, H. Ghassemian, Fusion of MS and PAN Images Preserving Spectral Quality, IEEE Geoscience and Remote Sensing Letters 12 (3) (2015) 611–615.

[5] R. A. Schowengerdt, Remote Sensing: Models and Methods for Image Processing, 2nd ed. Orlando, FL, USA: Academic, 1997

[6] J. Nunez et al., “Multiresolution-based image fusion with additive wavelet decomposition,” IEEE Trans. Geosci. Remote Sens., vol. 37, no. 3, pp. 1204–1211, May 1999.

[7] P.J. Burt, E.H. Adelson, The Laplacian pyramid as a compact image code, IEEE Transactions on Communications COM-31 (4) (1983) 532–540.

[8] R.H. Yuhas, A.F.H. Goetz, J.W. Boardman,Discrimination among semi-arid landscape endmembers using the Spectral Angle Mapper (SAM) algorithm, in: proceedings of Summaries of the Third Annual JPL Airborne Geoscience Workshop, 1992, pp.147–149.

[9] Z. Wang, A.C. Bovik, A universal image quality index, IEEE Signal Processing Letters 9 (3) (2002) 81–84.

[10] L. Alparone, S. Baronti, A. Garzelli, and F. Nencini, “A global quality measurement of pan-sharpened multispectral imagery,” IEEE GeosciRemote Sens. Lett., vol. 1, no. 4, pp. 313–317, Oct. 2004.

[11] A. Garzelli and F. Nencini, “Hypercomplex quality assessment of multi-/hyper-spectral images,” IEEE Geosci. Remote Sens. Lett., vol. 6, no. 4, pp. 662–665, Oct. 2009.

[12] Landsat7 ETM+ dataset available at: http://earthexplorer.usgs.gov

[13] Quick Bird dataset available at : http://glcfapp.glcf.umd.edu:8080/esdi/ftp?id=24402

[14] R Prema and Dr.M.G.Sumithra, “Gabour Wavelet Based Scale Transformation for Fabric Defect Detection” in International Conference on Technical and Green Textiles (ICTGT-2017), pp 138-141